Small aggregates can cause nitrite accumulation in one-stage partial nitritation and anammox

S.E. Vlaeminck[1*], A. Terada[2,5], B.F. Smets[2], H. De Clippeleir[1], T. Schaubroeck[1], M. Carballa[1,4], W. Verstraete[1]

[*] Corresponding author. Tel.: +32 9 264 59 76; Fax: +32 9 264 62 48
[1] Laboratory of Microbial Ecology and Technology (LabMET), Ghent University, Coupure Links 653, 9000 Gent, Belgium (siegfried.vlaeminck@ugent.be, haydee.declippeleir@ugent.be, thomas.schaubroeck@ugent.be, willy.verstraete@ugent.be)
[2] Department of Environmental Engineering, Technical University of Denmark (DTU), Miljoevej, Building 113, 2800 Kgs. Lyngby, Denmark (bfs@env.dtu.dk)
[4] Department of Chemical Engineering, School of Engineering, University of Santiago de Compostela, Rúa Lope Gómez de Marzoa, s/n, 15782 Santiago de Compostela, Spain (marta.carballa@usc.es)
[5] Department of Chemical Engineering, Tokyo University of Agriculture and Technology, 2-24-16 Naka-cho, Koganei-shi, Tokyo 184-8588, Japan (akte@cc.tuat.ac.jp)

Abstract
Aerobic and anoxic ammonium-oxidizing bacteria (AerAOB and AnAOB) cooperate in partial nitritation/anammox systems to remove ammonium from wastewater. In this process, nitrite accumulation is not desirable, since it decreases the nitrogen removal rate and since it can potentially inhibit the AnAOB. This study addressed several aspects of the microbial aggregate size for three independent types of suspended biomass, designated 'A', 'B' and 'C', for the first time including biomass from pilot- and full-scale applications. Firstly, the AerAOB and AnAOB abundance and the activity balance were quantified for the different aggregate sizes, separated in up to six size classes. Secondly, aggregate morphology, size distribution and architecture were examined. In all systems, the AerAOB abundance was highest in small aggregates (25-80% AerAOB; 1-21% AnAOB), while the AnAOB abundance was highest in large aggregates (1-36% AerAOB; 22-85% AnAOB). A nitrite accumulation rate ratio *(narr)* was defined as the net aerobic nitrite production rate divided by the anoxic nitrite consumption rate. The smallest 'A', 'B' and 'C' aggregates were nitrite sources *(narr* > 1.7). Large 'A' and 'C' aggregates were granules capable of autonomous nitrogen removal *(narr* 0.6-1.1) with internal AnAOB zones surrounded by an AerAOB rim. Large 'B' aggregates were thin film-like nitrite sinks *(narr* < 0.5) in which AnAOB were not shielded by an AerAOB layer. Overall, no unique, optimal aggregate size distribution or aggregate architecture was required to obtain good nitrogen removal in the three independent partial nitritation/anammox systems. Yet, selecting for larger aggregates can be an effective measure to prevent nitrite accumulation.

Keywords: confocal laser scanning microscope (CLSM), nitrification, OLAND

INTRODUCTION

In the last years, autotrophic nitrogen removal via partial nitritation and anoxic ammonium oxidation (anammox) has evolved from lab- to full-scale treatment of nitrogenous wastewaters with a low biodegradable organic content, mainly driven by a significant decrease of the operational costs compared to conventional nitrification and heterotrophic denitrification (Mulder, 2003; Fux and Siegrist, 2004). Oxygen-limited autotrophic nitrification/denitrification (OLAND) is one of these autotrophic processes, and is conducted in one stage, i.e. partial nitritation and anammox occurring in the same reactor (Pynaert et al., 2003). The 'functional' autotrophic micro-organisms in OLAND include aerobic and anoxic ammonium-oxidizing bacteria (AerAOB and AnAOB). With oxygen, AerAOB oxidize ammonium to nitrite (nitritation), and with the latter AnAOB oxidize the residual ammonium into dinitrogen gas and some nitrate (anammox). Additional aerobic nitrite oxidation to nitrate (nitratation) by nitrite-oxidizing bacteria (NOB) lowers the nitrogen removal efficiency, which can be prevented at low dissolved oxygen (DO) levels (Laanbroek and Gerards, 1993).

Reactor configurations for the OLAND process can be based on suspended biomass growing in aggregates, such as the sequencing batch reactor (SBR) (Vlaeminck et al., 2009a) and the gas-lift or upflow reactor (Sliekers et al., 2003). Suspended growth systems embrace two important challenges: biomass retention and equilibrated microbial activities. A high biomass retention efficiency is prerequisite in anammox-comprising technologies because of the slow growth of

AnAOB (Strous et al., 1998). Biomass settling properties determine the retention of biomass and are related to the microbial aggregate morphology (floc/granule) and size. In terms of physical properties, large granules are preferable for suspended-growth applications, since aerobic granules showed a lower sludge volume index compared to flocs, and an increase of the settling velocity with increasing granule size (Toh et al., 2003). OLAND aggregate size does not only influence settling properties but also affects the proportion of microbial nitrite production and consumption: for larger aggregates, a lower AerAOB and a higher AnAOB activity were shown (Vlaeminck et al., 2009a; Nielsen et al., 2005), as well as a broader optimal DO range for nitrogen removal (Volcke et al., in press). Hence, with an increasing aggregate size, and thus with a decreasing ratio of nitrite production to consumption, three functional categories of aggregates can be distinguished: nitrite sources, autonomous nitrogen removers (equal nitrite production and consumption) and nitrite sinks. Because minimal nitrite accumulation is one of the prerequisites for a high nitrogen removal efficiency in OLAND reactors, the excessive presence of small aggregates is undesirable (Vlaeminck et al., 2009a; De Clippeleir et al., 2009). For OLAND SBRs, effective removal of the smallest aggregates was recently demonstrated by applying shorter settling times (De Clippeleir et al., 2009), or by installing a cyclone (Wett et al., 2010).

The first objective of this study was to gain more insight in the relation between OLAND aggregate size, the AerAOB and AnAOB abundance and the activity balance. The second objective was to examine the process requirement for a certain aggregate size distribution, morphology and architecture. The different aspects were studied in three reactors designated ‘A’, ‘B’ and ‘C’ (Table 1), for the first time including OLAND applications treating real wastewater. The choice for these OLAND reactors was based on their differences in inoculation and operation (mixing and aeration). A digested domestic wastewater matrix has been shown not to influence the autotrophic community significantly (Vlaeminck et al., 2009b), and therefore minor influent differences in biodegradable organic carbon were assumed to have a minor effect on autotrophic activity ratios and architecture. Overall, this is the first study examining size related aspects of different types of suspended OLAND biomass with the same approach.

MATERIAL AND METHODS

Aerobic and anoxic batch activity tests

From the three studied systems ‘A’, ‘B’ and ‘C’ (Table 1), representative mixed liquor samples were obtained. Depending on the sample, the biomass was sieved in various size classes (pore sizes 0.10, 0.25, 0.50, 1.0, 1.6 and 2.0 mm) and washed with phosphate buffer (100 mg P L^{-1}, pH 8) to remove residual dissolved (in)organic compounds. Aerobic and anoxic activity tests were determined the day after biomass harvesting as previously described (Vlaeminck et al., 2007). In the aerobic test the presence of 1550 mg P L^{-1} minimized concurrent activity of AnAOB (Dapena-Mora et al., 2007).

Fluorescent in-situ *hybridization (FISH)*

FISH was performed to identify and visualize AerAOB, NOB and AnAOB, and to quantify AerAOB and AnAOB. Biomass was fixed in a 4% paraformaldehyde solution for 4 hours at 4°C. Large aggregates were embedded in OCT compound, cut in 20-µm slices with a cryomicrotome (−20°C) and attached to poly-L-lysine coated slides. FISH was performed according to Amann et al. (1990). An equimolar probe mixture of Nso1225 and Nso190 was used for the β-proteobacterial AerAOB, probe Amx820 for the AnAOB “*Candidatus* Brocadia and Kuenenia” and probe Ntspa662 with competitor for the NOB *Nitrospira* spp. Probe sequences and formamide concentrations were applied according to probeBase (Loy et al., 2003), unless for the equimolar mixture of Nso1225 and Nso190, 35% formamide was applied (Pynaert et al., 2003). The qualitative or quantitative presence of the target was evaluated by combining the specific probe with an equimolar mixture of EUB338I, II and III, targeting all bacteria (Loy et al., 2003). Probe

fluorochromes were FLUO, Cy3 or Cy5. For quantification and architecture visualisation, image acquisition was done on a Leica TCM SP5 confocal laser scanning microscope (CLSM; Leica Microsystems, Wetzlar, Germany). Ten CLSM image stacks (10 µm depth, 3 heights) were analyzed with Daime software (Daims et al., 2006), and the percentage of AerAOB and AnAOB was calculated as the ratio of the specific to the total bacterial biovolume. The architecture was also examined on a Zeiss Axioskop 2 Plus epifluorescence microscope (Carl Zeiss, Jena, Germany).

Table 1. Overview of the three OLAND reactor systems from which suspended biomass was sampled. Aggregates settling at a higher rate than the minimum settling velocity (MSV) were not washed out from the sequencing batch reactors (SBRs). COD: chemical oxygen demand; DO: dissolved oxygen.

Biomass label	'A'	'B'	'C'
Reactor type	SBR	SBR	Upflow reactor
Volume (m^3)	0.002	4.1	600
Reactor height/diameter (m m^{-1})	0.9	4	0.5-0.8
Inoculum	OLAND biofilm	Activated sludge	Anammox granules
Wastewater	Synthetic	Domestic[a]	Industrial[b]
Influent ammonium (mg N L^{-1})	230-330	800	250-350
Nitrogen removal rate (g N L^{-1} d^{-1})	0.45[c]; 1.1[d]	0.65	1.3
Effluent nitrite (mg N L^{-1})	30-40[c]	5-10	5-10
Effluent ammonium (mg N L^{-1})	> 20	> 10	> 10
Influent/effluent COD (mg L^{-1})	0/0	240/220	200/150
pH	7.4-7.8	7.4-7.6	8.0
Temperature (°C)	35	25	30-35
DO level (mg O_2 L^{-1})	0.4-1.1	0.5-1.0	2.0-3.0
Mixing mechanism	Magnetic stirrer	Bladed impeller	Aeration
Biomass retention mechanism	MSV > 0.73 m h^{-1}	MSV > 1.4 m h^{-1}	3-phase separator
Sampling time (months after start-up)	2[c]	8	30

[a] Supernatant from municipal sludge digestor (Jeanningros et al., 2010)
[b] Effluent from potato processing factory pretreated with anaerobic digestion and struvite precipitation (Abma et al., 2010)
[c] Obtained at the end of a reactor start-up study (Vlaeminck et al., 2009a)
[d] Obtained at the end of a reactor start-up study (De Clippeleir et al., 2009)

Chemical analyses

Nitrite and nitrate were determined on a 761 Compact Ion Chromatograph equipped with a conductivity detector (Metrohm, Zofingen, Switzerland). Ammonium (Nessler method), chemical oxygen demand (COD; dichromate method) and VSS (weighing and drying) were determined according to standard methods (Greenberg et al., 1992). pH was measured potentiometrically, and DO concentration and water temperature were monitored with a COM381 DO meter (Endress-Hauser, Reinach, Switzerland).

RESULTS

Aggregate size and activity

The three types of suspended biomass 'A', 'B' and 'C' (Table 1), displayed different morphologies and size distributions. Biomass 'A' consisted of two fractions with a divergent size: granular aggregates, all exceeding 1 mm (Fig. 1.I), and floccular aggregates, collected on a 0.10 mm sieve (Fig. 1.II). Particle sizes of 'B' were less divergent, allowing to divide the biomass in four size classes (Fig. 1.III). Since 90% of 'C' was larger than 1 mm, this biomass was sieved in six size classes.

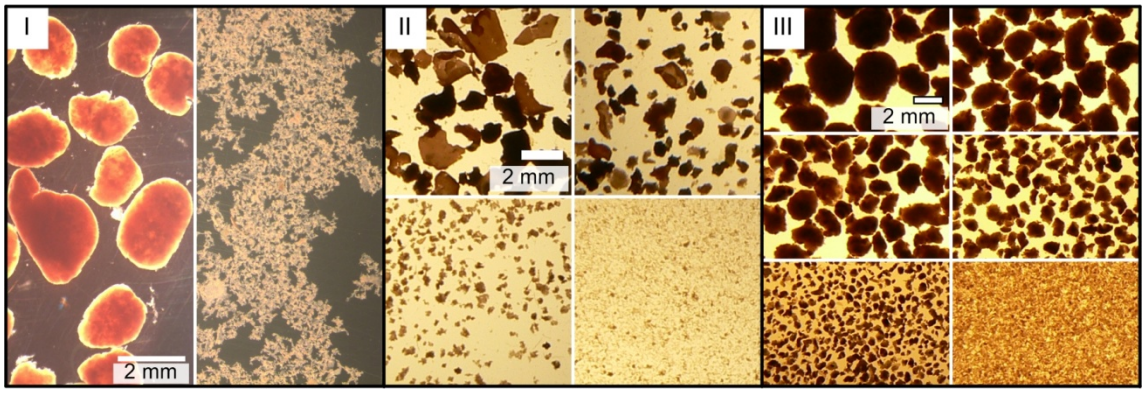

Figure 1. Micrographs of the suspended biomass after separation in different size classes: biomass 'A' (panel I), 'B' (panel II) and 'C' (panels III).

In the three reactor systems, the AerAOB activity rate decreased and the AerAOB abundance was lower with increasing aggregate size, whereas the opposite was true for the AnAOB activity and abundance (Table 2). In 'A' and 'B', no NOB activity was detected. In 'C', the NOB activity decreased with increasing size from 0.25 mm on. To evaluate the autotrophic nitrite accumulation potential of an aggregate or a mixture of aggregates, a dimensionless nitrite accumulation rate ratio *(narr)* was calculated by dividing the net nitrite production rate by the nitrite consumption rate (eq. 1).

$$\text{Nitrite accumulation rate ratio } (narr) = \frac{\text{AerAOB } NO_2^- \text{ production rate} - \text{NOB } NO_2^- \text{ consumption rate}}{\text{AnAOB } NO_2^- \text{ consumption rate}} \quad \text{(eq. 1)}$$

Large 'A' (> 1.0 mm) and 'C' (>0.50 mm) aggregates had *narr* values close to 1 (Table 2). In all reactors, the highest *narr* values corresponded to the smallest aggregates, whereas the lowest *narr* values were obtained for the larger 'B' aggregates (> 0.25 mm) (Table 2). Taking into account the relative abundance of each size class, the *narr* values for the mixed biomass were 2.3 ('A'), 1.2 ('B') and 0.93 ('C').

Autotrophic aggregate architecture

Aggregate appearance differed per reactor system, especially for the large aggregates which were globular and rigid granules in 'A' (Fig. 1.I) and 'C' (Fig. 1.III), and planar and flexible film-like structures in 'B' (Fig. 1.II).

In the smallest biomass fractions (0.10-0.25 mm), the autotrophs mostly appeared as spherical microcolonies. In 'A' and 'B', AnAOB clusters were positioned close to AerAOB clusters (Fig. 2.I, 2.III), and the AnAOB abundance was higher in 'B' compared to 'A' (Table 2). In 'C', almost no AnAOB were detected in the smallest biomass fraction (Table 2), and *Nitrospira* spp. microcolonies were larger than and positioned closely to AerAOB microcolonies (Fig. 2.V).

Thin sections showed that the 'A' granular architecture consisted of an AerAOB rim and many internal parallel AerAOB layers in which AnAOB zones were embedded (Fig. 2.II). The thickness of the AerAOB rim ranged from 24 ± 6 to 43 ± 8 µm (n = 15). Internal AerAOB bands were 16 ± 4 µm (n = 32) thick, interspaced at 14 ± 5 µm (n = 32). The different directions of parallel AerAOB bands in co-sectioned granules demonstrated that the bands were not a compaction artefact of cryomicrotome sectioning (data not shown). The AnAOB were heterogeneously spread over the granule section, appearing as spherical microcolonies (data not shown) or as pleomorphic zones.

Table 2. Activity of AerAOB, NOB and AnAOB according to aggregate size, as determined in batch activity tests (n = 1 for 'A'; n = 3 for 'B' and 'C'). The AnAOB nitrite consumption per ammonium consumption derived from AnAOB batch tests slightly differed per reactor system ('A': 1.17; 'B': 1.11 ± 0.02; 'C' = 1.13 ± 0.02), but was not affected by the aggregate size. Calculation and interpretation of the nitrite accumulation rate ratio *(narr)* is described in the 'Results' section. AerAOB and AnAOB abundance were quantified with FISH and expressed as a percentage of the total bacterial volume. Activities and abundances are expressed as averages ± standard deviation. VSS: volatile suspended solids; '-': not determined.

	Biomass 'A'		Biomass 'B'				Biomass 'C'					
Aggregate size (mm)	0.1-1.0	>1.0	0.1-0.25	0.25-0.5	0.5-1.0	>1.0	0.1-0.25	0.25-0.5	0.5-1.0	1.0-1.6	1.6-2.0	>2.0
% of total VSS	43	57	77	10	6	7	2.7	1.0	6.7	35	35	20
NH_4^+ consumption rate by AerAOB (mg NH_4^+-N g VSS^{-1} d^{-1})	426	110	191 ± 20	85 ± 2	32 ± 2	21 ± 13	1040 ± 86	200 ± 35	218 ± 21	209 ± 12	173 ± 31	159 ± 17
NO_3^- production rate by NOB (mg NO_3^--N g VSS^{-1} d^{-1})	0	0	0	0	0	0	37 ± 15	72 ± 8	56 ± 11	47 ± 1	45 ± 11	36 ± 2
NH_4^+ consumption rate by AnAOB (mg NH_4^+-N g VSS^{-1} d^{-1})	36	133	99 ± 5	172 ± 2	159 ± 5	191 ± 8	5.6 ± 4.6	103 ± 26	163 ± 11	156 ± 13	161 ± 15	171 ± 9
Narr (-)	10	0.70	1.7	0.44	0.18	0.10	158	1.1	0.88	0.92	0.70	0.63
AerAOB abundance (%)	80 ± 7	36 ± 9	25 ± 4	-	-	1.1 ± 0.6	29 ± 11	-	-	-	4.9 ± 1.5	-
AnAOB abundance (%)	6.0 ± 0.9	22 ± 8	21 ± 6	-	-	85 ± 8	1.3 ± 8.9	-	-	-	69 ± 7	-

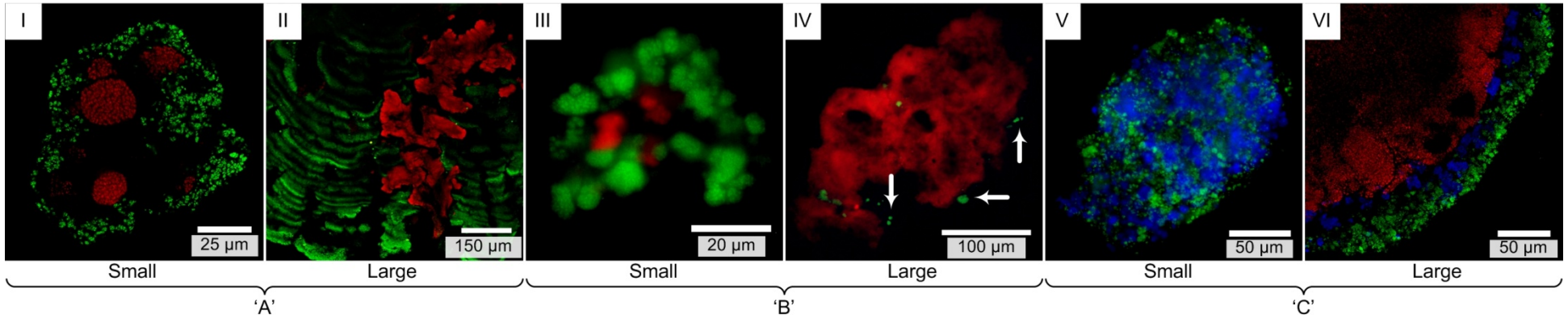

Figure 2. FISH micrographs for small and large aggregates of the biomass types 'A', 'B' and 'C'. AerAOB (Nso1225 and Nso190) are displayed in green, *Nitrospira* spp. (Ntspa662) in blue and AnAOB (Amx820) in red. **I.** Floc with AerAOB and AnAOB microcolonies. **II.** Granule with pleomorphic AnAOB zones embedded in parallel AerAOB bands. **III.** Floc with AerAOB and AnAOB microcolonies. **IV.** Large aggregate with some AerAOB microcolonies (examples with arrows) on the AnAOB core. **V.** Floc with AerAOB and NOB microcolonies. **VI.** Three-layered granule stratification: AerAOB, *Nitrospira* spp. and AnAOB.

In contrast to 'A', AnAOB were not surrounded by AerAOB in large 'B' aggregates. Sections showed an AnAOB zone with only some scattered AerAOB microcolonies on the edge (Fig. 2.IV). Irregularly shaped void spaces of up to ca. 50 by 50 µm occupied 13 ± 5% (n = 10) of the combined AnAOB and voids area. No cells were present in these voids (data not shown).

'C' granules consisted of an AerAOB rim, similar to 'A', a subsequent *Nitrospira* spp. layer, and an AnAOB core (Fig. 2.VI). The AerAOB rim ranged from 20 ± 7 to 35 ± 12 µm (n = 15), and the combined aerobic layer (AerAOB and NOB) from 30 ± 11 to 65 ± 17 µm (n = 15), which is roughly 20 µm thicker than the AerAOB rim of 'A' granules. Similar to 'B', the AnAOB zone contained irregularly shaped voids/channels up to ca. 50 by 150 µm, occupying 17 ± 4% (n = 10) of the combined AnAOB and voids zone. No cells were present in the voids (data not shown).

DISCUSSION

The first objective of this study was to relate the AerAOB and AnAOB abundance and the activity balance to the size of OLAND aggregates. Activity and abundance of AerAOB (resp. AnAOB) were lower (resp. higher) with increasing aggregate size. The activity balance was evaluated in terms of nitrite production and consumption, and was condensed into the dimensionless parameter *narr*. The validity of *narr* depends on two assumptions: (i) the ratio of the activity rates determined in batch can be extrapolated to the *in-situ* reactor activity, and (ii) in case of NOB activity, NOB preferentially consume the nitrite before the AnAOB given their close juxtaposition to the nitrite producers (AerAOB). Based on the *narr* definition (eq. 1), the functional categories of nitrite sources, autonomous nitrogen removers and nitrite sinks can be attributed to *narr* values which are considerably below 1, around 1 and considerably above 1, respectively. The relation between the functional category and the size of an aggregate, was dependent on the examined system. 'A' and 'C' granules had a *narr* value around 1 and could autonomously obtain nitrogen removal, without excessive aerobic nitrite production or severe anoxic nitrite limitation. Similarly, the large flocs obtained by Nielsen et al. (2005) (> 0.50 mm) were autonomous nitrogen removers, given their *narr* value of 1.1. In contrast, large 'B' aggregates were nitrite sinks, and all the small aggregates were nitrite sources. It suggests that nitrite sources had to feed nitrite sinks to obtain nitrogen removal in 'B'. *Narr* was also calculated for the complete reactor system. The high value of system 'A' *(narr* = 2.3) corresponded well with the relatively high nitrite values in the reactor's effluent (Table 1). Overall, *narr* can be easily determined and is a useful tool to evaluate the OLAND activity balance of an aggregate (mixture) in a dimensionless way. It should be noted that optimization of a oxygen-limited batch test protocol is desirable to further improve realistic extrapolation from batch activity results to nitrogen removal performance on a reactor scale.

The second objective of this study was to link the similar nitrogen removal performance of 'A', 'B' and 'C' (Table 1) to similarities in aggregate size distributions (Table 2), aggregate morphology (Figure 1) and architecture (Figure 2). Since these parameters were quite different for every system, however, no apparent unique aggregate properties were required to obtain good nitrogen removal. Instead, reactor-specific differences likely gave rise to the observed differences in the biomass properties, as elaborated in the following paragraphs.

In 'A' granules, internal AerAOB layers (Fig. 2.II) probably derived from the type of inoculum, i.e. biofilm grown on rotating discs, since the same structures were observed there (Vlaeminck et al., 2009b). The lowest specific aerobic activity was measured in 'A' granules (306 mg N g^{-1} AerAOB-VSS^{-1} d^{-1}), indicating that the AerAOB in the anoxic core could not grow aerobically. Compared to the inoculum biofilm, the anoxic activity of the granules was 6 times higher (Vlaeminck et al., 2009a), showing AnAOB growth in the anoxic granule core.

The spatial distribution of dissolved oxygen determines where AerAOB and AnAOB can grow, since oxygen is an AerAOB substrate and an AnAOB inhibitor (Strous et al., 1997). In systems 'A' and 'C', the granular aerobic rim could create anoxic conditions on a micro scale (order 50-100 μm). In contrast, large 'B' aggregates were not surrounded by AerAOB, probably due to oxygen gradients on a macro (reactor) scale. Gentle impeller mixing and a large height/diameter ratio of the reactor (Table 1) were likely factors rendering a heterogeneous, incomplete mixing. As such, large aggregates could settle in hydraulically 'dead', anoxic reactor corners, allowing for AnAOB growth without the need for an AerAOB 'shield'.

In reactor 'C', the relatively high DO levels (Table 1) can explain the high NOB activity rates throughout all size classes as well as the low AnAOB activity rate in the smallest aggregates. NOB activity accounted for 21% of the AerAOB rate in the overall 'C' sample. In the likely case the NOB oxygen affinity constant exceeded the AerAOB counterpart (Laanbroek and Gerards, 1993), an important decrease of the DO level would allow the AerAOB to outcompete the NOB, increasing the overall nitrogen removal efficiency. Further, calculation based on the measured aerobic activity shows that a DO decrease from 2.5 to 0.75 mg O_2 L^{-1} decreases the radial oxygen penetration depth in the smallest aggregates from 96 to 52 μm, assuming zero-order substrate uptake (Perez et al., 2005). The deep oxygen penetration at the high DO level explains the low AnAOB abundance (1%, Table 2), and the anoxic zones generated by a DO decrease would allow for AnAOB proliferation, lowering the extremely high *narr* value of 158.

Besides species-specific growth, decay is also considered to play a role in the mature granule architecture. Large 'B' and 'C' aggregates were AnAOB-rich (85 and 69%), but their AnAOB-specific removal rates (224 and 233 mg N g^{-1} AnAOB-VSS^{-1} d^{-1}) were at least around two times lower than in the other AnAOB-quantified biomass (430-605 mg N g^{-1} AnAOB-VSS^{-1} d^{-1}). It follows that part of the AnAOB in AnAOB-rich aggregates were substrate limited. Subsequent decay could give rise to the formation of voids occupying 13 to 17% of the anoxic zone.

CONCLUSIONS

Three suspended OLAND systems with comparable nitrogen removal rates and different inoculum, influent and operation conditions, showed a different *narr* distribution with aggregate size corresponding to the respective aggregate architectures. To obtain good nitrogen removal, no unique, optimal aggregate size distribution was required. Yet, a decreased abundance of the smallest aggregates in the system can prevent nitrite accumulation.

ACKNOWLEDGMENTS

S.E.V. was supported as a postdoctoral fellow from the Research Foundation Flanders (FWO-Vlaanderen), H.D.C. was recipient of a PhD grant from the Institute for the Promotion of Innovation by Science and Technology in Flanders (IWT-Vlaanderen, number SB-81068), M.C. received a postdoctoral contract for Dr. Marta Carballa from the 'Xunta de Galicia' (Isidro Parga Pondal program, IPP-08-37). Work at DTU was supported by a research grant (FTP-ReSCoBiR) from the 'Danish agency for Science Technology and Innovation' (Research Council for Technology & Production, FTP). We would like to express our utmost gratitude to Wiebe Abma (Paques, Balk, the Netherlands) and Dr. Laure Graveleau (Degrémont, Rueil Malmaison, France) for the very kind provision of biomass.

References

Mulder, A. (2003) The quest for sustainable nitrogen removal technologies. Water Science and Technology 48(1), 67-75.

Fux, C. and Siegrist, H. (2004) Nitrogen removal from sludge digester liquids by nitrification/denitrification or partial nitritation/anammox: environmental and economical considerations. Water Science and Technology 50(10), 19-26.

Pynaert, K., Smets, B.F., Wyffels, S., Beheydt, D., Siciliano, S.D. and Verstraete, W. (2003) Characterization of an autotrophic nitrogen-removing biofilm from a highly loaded lab-scale rotating biological contactor. Applied and Environmental Microbiology 69(6), 3626-3635.

Laanbroek, H.J. and Gerards, S. (1993) Competition for limiting amounts of oxygen between *Nitrosomonas europaea* and *Nitrobacter winogradskyi* grown in mixed continuous cultures. Archives of Microbiology 159(5), 453-459.

Vlaeminck, S.E., Cloetens, L.F.F., Carballa, M., Boon, N. and Verstraete, W. (2009a) Granular biomass capable of partial nitritation and anammox (vol 58, pg 1113, 2008). Water Science and Technology 59(3), 609-617.

Sliekers, A.O., Third, K.A., Abma, W., Kuenen, J.G. and Jetten, M.S.M. (2003) CANON and Anammox in a gas-lift reactor. FEMS Microbiology Letters 218(2), 339-344.

Strous, M., Heijnen, J.J., Kuenen, J.G. and Jetten, M.S.M. (1998) The sequencing batch reactor as a powerful tool for the study of slowly growing anaerobic ammonium-oxidizing microorganisms. Applied Microbiology and Biotechnology 50(5), 589-596.

Toh, S.K., Tay, J.H., Moy, B.Y.P., Ivanov, V. and Tay, S.T.L. (2003) Size-effect on the physical characteristics of the aerobic granule in a SBR. Applied Microbiology and Biotechnology 60(6), 687-695.

Nielsen, M., Bollmann, A., Sliekers, O., Jetten, M., Schmid, M., Strous, M., Schmidt, I., Larsen, L.H., Nielsen, L.P. and Revsbech, N.P. (2005) Kinetics, diffusional limitation and microscale distribution of chemistry and organisms in a CANON reactor. FEMS Microbiology Ecology 51(2), 247-256.

Volcke, E.I.P., Picioreanu, C., De Baets, B. and van Loosdrecht, M.C.M. (in press) Effect of granule size on autotrophic nitrogen removal in a granular sludge reactor. Environmental Technology.

De Clippeleir, H., Vlaeminck, S.E., Carballa, M. and Verstraete, W. (2009) A low volumetric exchange ratio allows high autotrophic nitrogen removal in a sequencing batch reactor. Bioresource Technology 100(21), 5010-5015.

Wett, B., Hell, M., Nyhuis, G., Puempel, T., Takacs, I. and Murthy, S. (2010) Syntrophy of aerobic and anaerobic ammonia oxidisers. Water Science and Technology 61(8), 1915-1922.

Vlaeminck, S.E., Terada, A., Smets, B.F., Van der Linden, D., Boon, N., Verstraete, W. and Carballa, M. (2009b) Nitrogen Removal from Digested Black Water by One-Stage Partial Nitritation and Anammox. Environmental Science & Technology 43(13), 5035-5041.

Vlaeminck, S.E., Geets, J., Vervaeren, H., Boon, N. and Verstraete, W. (2007) Reactivation of aerobic and anaerobic ammonium oxidizers in OLAND biomass after long-term storage. Applied Microbiology and Biotechnology 74(6), 1376-1384.

Dapena-Mora, A., Fernandez, I., Campos, J.L., Mosquera-Corral, A., Mendez, R. and Jetten, M.S.M. (2007) Evaluation of activity and inhibition effects on Anammox process by batch tests based on the nitrogen gas production. Enzyme and Microbial Technology 40(4), 859-865.

Amann, R.I., Krumholz, L. and Stahl, D.A. (1990) Fluorescent-oligonucleotide probing of whole cells for determinative, phylogenetic, and environmental studies in microbiology. Journal of Bacteriology 172(2), 762-770.

Loy, A., Horn, M. and Wagner, M. (2003) probeBase: an online resource for rRNA-targeted oligonucleotide probes. Nucleic Acids Research 31(1), 514-516.

Daims, H., Lucker, S. and Wagner, M. (2006) daime, a novel image analysis program for microbial ecology and biofilm research. Environmental Microbiology 8(2), 200-213.

Jeanningros, Y., Vlaeminck, S.E., Kaldate, A., Verstraete, W. and Graveleau, L. (2010) Fast start-up of a pilot-scale deammonification sequencing batch reactor from an activated sludge inoculum. Water Science and Technology 61(6), 1393-1400.

Abma, W.R., Driessen, W., Haarhuis, R. and van Loosdrecht, M.C.M. (2010) Upgrading of sewage treatment plant by sustainable and cost-effective separate treatment of industrial wastewater. Water Science and Technology 61(7), 1715-1722.

Greenberg, A.E., Clesceri, L.S. and Eaton, A.D. (1992) Standard Methods for the Examination of Water and Wastewater, American Public Health Association, Washington DC.

Strous, M., van Gerven, E., Kuenen, J.G. and Jetten, M. (1997) Effects of aerobic and microaerobic conditions on anaerobic ammonium-oxidizing (Anammox) sludge. Applied and Environmental Microbiology 63(6), 2446-2448.

Perez, J., Picioreanu, C. and van Loosdrecht, M. (2005) Modeling biofilm and floc diffusion processes based on analytical solution of reaction-diffusion equations. Water Research 39(7), 1311-1323.